A Safety Strategy for Producing Poly(Acrylic Acid) of Low Molar Mass

Gerardo Cáceres Montenegro, Carolina G. Gutierrez, Santiago E. Vaillard, Roque J. Minari, Jorge R. Vega, Luis M. Gugliotta*

The synthesis of poly(acrylic acid) (PAA) of low molar mass under safe conditions is difficult due to the high polymerization rate of acrylic acid (AA) and the fast heat generation. The aqueous-solution "semibatch" polymerization of non-ionized AA in almost starved conditions involves high initiator loads when low molar masses are required. This article proposes the simultaneous feeding of AA and nonconventional chain transfer agents (CTA) as a strategy aimed at controlling both the molar masses and the generated heat rate. Three CTAs are investigated: 2-mercaptoethanol, thioglycolic acid, and isopropyl alcohol. Even when PAA of relatively low molar mass can be produced by adequately selecting the flow rates and concentrations of both AA and CTA, it is found that the nature of CTA can have a significant effect on the polymerizations kinetics. The mechanisms responsible for these effects are discussed with the help of a representative mathematical model.

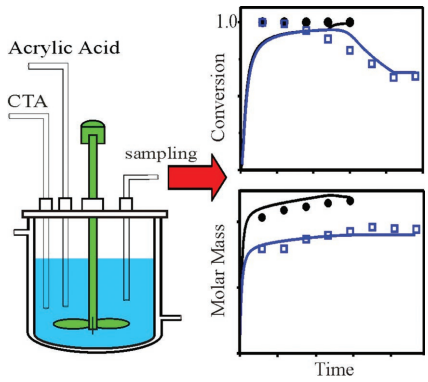

1. Introduction

Since poly(acrylic acid) (PAA) is a weak polyelectrolyte, its degree of ionization varies with pH. Solutions of PAA have interesting properties because the structure of the polymer varies with the degree of ionization, the medium ionic strength, and the nature of the counterions.[1–3] PAA and its polyacrylates derivatives are quite versatile for many applications. They are widely used as scale inhibitors, clay deflocculants,[4] superabsorbents,[5] antimicrobial agents,[6] adsorbents in wastewater treatment,[7,8] biomedical applications,[9] and cosmetic additives.[10]

PAA is employed in the ceramic industry as deflocculating and spreading agent, where its molecular microstructure must be fine-tuned to ensure an adequate performance. A PAA of medium or low molar mass (MM) (<100 kDa) is often used as deflocculant agent, while a PAA of high MM (>800 kDa) is used as flocculant agent.

PAA of medium or low MM is mainly produced through a radical polymerization of AA in aqueous solution. The high reactivity of AA (the propagation rate constant at 60 °C in acid media is 8.7×10^6 mol min^{-1} L^{-1}, around 300 times higher than styrene homopropagation at the same temperature), and its high exothermicity (heat of polymerization ΔH_{AA} = 77.5 kJ mol^{-1}) make difficult the production of PAA with a prespecified MM and under thermal controllability to ensure process reproducibility.

Dr. G. C. Montenegro
Departamento de Química Orgánica
Universidad de Panamá
Ciudad Universitaria
Via Simón Bolivar 0819, Panamá
Dr. G. C. Montenegro, Dr. C. G. Gutierrez, Dr. S. E. Vaillard, Dr. R. J. Minari, Prof. J. R. Vega, Prof. L. M. Gugliotta
INTEC (CONICET – Universidad Nacional del Litoral)
Güemes 3450, Santa Fe 3000, Argentina
E-mail: lgug@intec.unl.edu.ar
Dr. R. J. Minari, Prof. L. M. Gugliotta
Facultad de Ingeniería Química (Universidad Nacional del Litoral)
Santiago del Estero 2829, Santa Fe 3000, Argentina
Prof. J. R. Vega
Facultad Regional Santa Fe (Universidad Tecnológica Nacional)
Lavaisse 610, Santa Fe 3000, Argentina

Macromol. React. Eng. **2017**, DOI: 10.1002/mren.201600049

The kinetics of AA polymerization is quite complex due to backbiting reactions (1,5 hydrogen shift), which transform the secondary propagating radical (SPR) into a less reactive tertiary mid-chain radical (MCR).[11] MCRs can add monomer and thus be retransformed into SPRs.

The polymerization rate of AA and the MM of the obtained PAA strongly depend on experimental conditions,[12,13] such as the selected type of process, the solids content, the reaction temperature, the initiation system (dissociative or redox), the degree of neutralization, the medium conditions (pH and ionic strength), and the use of chain transfer agents (CTAs).

The increasing demand of PAA of low MM from various industrial applications (civil engineering, household chemistry, wastewater treatment, textile, ceramics, and leather) has motivated a strong interest for investigating the chemical processes to produce such polymers.[14–17] In a previous work, an AA feeding strategy was proposed to produce PAA of controlled MM (between 10 and 200 kDa), at complete AA conversion and under safe conditions.[18] With this strategy, a high concentration of potassium persulfate (KPS) was required to produced PAA of relatively low MM, while no significant MM reduction was obtained when the KPS concentration exceeded a limit of 3% weight based on monomer.[18] On the other hand, CTAs are normally used for reducing the MM, but water soluble CTAs have been mainly investigated in batch processes.[19] Typically, the chemical structure of CTAs includes thiols, amines, secondary alcohols (e.g., isopropyl alcohol), bisulfite ion, monobasic sodium phosphate, thiol acids (e.g., 2-mercaptoethanol or thioglycolic acid),[20] and alkyl halides.[21] Thiols are usually employed as CTAs because they exhibit high chain transfer constants, while aldehydes or alcohols are weaker CTAs.[22]

In some cases, when the radical function is transferred to CTAs, the rate of polymerization can be altered due to the lower reactivity of the transferred radicals with respect to the propagating radicals; but being still capable of reinitiating the polymerization by a reaction termed retardation or degradative chain transfer.[23] In addition, there is evidence of redox couplings between thiol and persulfate, which can compete with the thermal initiation in the polymerization of acrylates carried out in batch mode with persulfates and/or bromates as initiators and in the presence of water soluble thiols (such as thiourea, thiomalic acid, 2-aminoethanethiol chloride, or α-mercaptocarboxylic acids).[24–26]

This work investigates the semibatch aqueous solution polymerization of AA in the presence of three different CTAs [mercaptoethanol (ME), thioglycolic acid (TGA), or isopropyl alcohol (IPA)] with the aim of safely producing PAA of controlled average MM in low range values. The ability of each CTAs to control the PAA molecular structure (measured as average MM and branching) as well as its influence on the polymerization kinetics are analyzed. A mathematical model that contains the main kinetic aspects of the aqueous solution polymerization of AA in presence of water soluble CTAs is developed to help interpreting the experimental data.

2. Experimental Section

2.1. Materials

All reagents were used as received. Polymerization reactions were carried out with AA [Aldrich, inhibited with 200 ppm of methylhydroquinone] and $K_2S_2O_8$ (KPS, Anedra, 99% purity) as initiator. The employed CTAs were ME (Fluka AG, >99% purity), TGA (Baker, purity 99%), and IPA (Cicarelli, purity 99%). Hydroquinone (Fluka AG, >99% purity) was employed as polymerization inhibitor. The MMs of all polymer samples were determined by size exclusion chromatography (SEC). The MM calibration was determined on the basis of a set of 12 PAA narrow standards (American Polymer Standard Corp., MM range 900–193 800 g mol^{-1}). The following reagents were used to prepare the eluent for SEC: NaH_2PO_4/$NaHPO_4$, $NaNO_3$ (to adjust ionic strength) and NaN_3 (to inhibit microbial growth). All SEC reagents were from Cicarelli Argentina (purity>98%). Distilled and deionized water was used throughout the work.

2.2. Polymerizations

Polymerization reactions were carried out at 70 °C in a semibatch reactor under semistarved conditions with the objective of maintaining low concentrations of AA in the reaction system during the entire operation thus working under safe conditions. The strategy consists of preloading the reactor with the initiator solution (KPS) and feeding the aqueous solutions of AA and CTA at low constant flow rates in separate streams, with the aim of simultaneously controlling the reaction temperature and the molar mass distribution (MMD). For all investigated reactions, the experimental conditions, the recipes, and the employed CTA/AA molar ratios are summarized in the upper part of Table 1.

A control reaction (CR) was carried out in absence of CTA. The other eight reactions are labeled with the abbreviation of the employed CTA followed by the experiment number. ME1-3, TGA1-3, and IPA1-2, were carried out with semicontinuous addition of CTA. Experiments ME1 and ME2 were similar to CR, but two different concentrations of ME were used; while lower concentrations of CTA and KPS were used in ME3. It should be noted that TGA1, TGA2, and TGA3 involved the same recipes but different AA and TGA feeding times ($t_{feeding}$) and total reaction time (t_r). Also note that the same moles of CTA were fed in TGA1-3, ME2, and IPA1. Finally, the CTA concentration in the IPA2 reaction was tenfold with respect to IPA1.

2.3. Sampling and Characterization

Samples were withdrawn along the polymerizations for measuring the total and fractional monomer conversions (x and x_f

Macromol. React. Eng. 2017, DOI: 10.1002/mren.201600049

Table 1. Semibatch polymerizations of AA (at 70 °C): reaction conditions (top), recipes (middle), and main characteristics of the final product (bottom).

Reactions	CR[a)]	ME1	ME2	ME3	TGA1	TGA2	TGA3	IPA1	IPA2
t_r [min]	150	150	150	150	240	150	150	150	150
$t_{feeding}$ [min]	120	120	120	120	210	120	60	120	120
AA [g]	79.5	79.5	79.5	79.5	79.5	79.5	79.5	79.5	79.5
KPS [g]	4.9	4.9	4.9	2.45	4.9	4.9	4.9	4.9	4.9
CTA [g]	0	0.90	1.38	0.45	1.62	1.62	1.62	1.06	10.6
Water [g]	315.6	314.7	314.2	317.6	314.0	314.0	314.0	314.5	305.0
Weight [g]	400	400	400	400	400	400	400	400	400
CTA/AA[b)] [–]	0	0.010	0.016	0.005	0.016	0.016	0.016	0.016	0.16
x [%]	100	100	73.5	94.9	63.5	88.3	99.6	100	100
$\bar{M}_n$ [kDa]	20.9	10.8	8.9	22.3	7.5	7.4	12.1	18.4	15.1
$\bar{M}_w$ [kDa]	58.8	30.5	24.2	65.6	18.6	21.7	26.0	52.8	37.4
D_n[c)] (–)	2.8	2.8	2.7	2.9	2.5	2.9	2.1	2.9	2.5
pH (–)	1.56	1.54	1.54	1.53	1.52	1.47	1.48	1.53	1.43

[a)]Control reaction without CTA; [b)]Molar ratio; [c)]$D_n = M_w/M_n$.

respectively), the MMD and their number- and weight-averages molar masses ($\bar{M}_n$ and $\bar{M}_w$). Monomer conversions were gravimetrically measured after drying the samples until constant weight at 70 °C.

PAA samples were analyzed by SEC. The chromatographic system involved a Waters 1515 isocratic pump, fitted with a set of five Ultrahydrogel (Waters) columns of nominal fractionation range 5×10^3 to 7×10^6 g mol^{-1}, and a Waters 2414 differential refractometer (DR). The MMD was estimated by combining the corrected DR chromatograms with the molar mass calibration determined with PAA narrow standards. The following aqueous buffer solution was used as eluent: $NaH_2PO_4/NaHPO_4$ 50×10^{-3} M (pH = 7) + $NaNO_3$ 50×10^{-3} M, at a flow rate of 0.8 mL min^{-1}. An injection loop of 200 μL was used. Samples for SEC were prepared from PAA solution directly taken from the reactor and diluted in the eluent buffer at a concentration of around 5 mg mL^{-1}. These relatively high concentrations were selected to improve the signal-to-noise ratio and the baseline definition at high elution volumes, where the solvent peaks can strongly distort the sample chromatograms. The measured signals were treated through an ad hoc data processing routine that was specially developed to compensate for artifacts introduced by the column overloading due to the required high-concentration injections (i.e., all chromatograms are shifted to higher elution volume and are additional broadened).[27]

The final samples were also characterized by gel phase ^{13}C NMR (Bruker Advance II 300 spectrometer, 75 MHz) in order to quantify the mean branching degree (BD) and elucidate the main kinetic mechanisms involved in the reactions.[18] NMR characterization was carried out on final PAA liquid samples (0.4 mL) containing D_2O (0.5–0.1 mL) in 5 mm NMR tubes. The BD was calculated through

$$BD(\%) = \frac{A(Cq)}{A(C=O)} 100 \quad (1)$$

where A(Cq) and A(C = 0) are the peak areas of the quaternary carbon (48 ppm) and carbonyl carbons linked to the main chain (172–180 ppm), respectively. According to Equation (1), BD represents the branching degree as the percentage of polymerized repeat units which contain a branching point.

3. Kinetics and Mathematical Model

The developed mathematical model is based on that presented by Minari et al.,[18] and describes the kinetics of the free radical solution polymerization of AA. An overview of the relevant reactions is presented in Table 2. Inherent assumptions in the polymerization mechanism are: i) thermal decomposition of KPS (Equation (2)), ii) generation of secondary radicals produced by the reaction of the monomer with sulfate radicals [the first and second indexes between brackets in $R^{\bullet}_{sec}(s,l)$ indicates the number of quaternary carbons linked to a short (s) branch and to a long (l) branch, respectively] (Equation (3)); iii) the generated secondary radicals can propagate with AA (Equation (4)), or can terminate (by combination) between them (Equation (5)), iv) chain transfer reaction between the secondary radicals and the CTA (Equation (6)), v) redox decomposition of the water soluble CTAs containing –SH groups (TGA and ME) with KPS, when they are employed, generating sulfate and mercaptan radicals ($RS^{\bullet}$ or $R^{\bullet}_{CTA}$)[28] (Equation (7)), vi) generation of CTA radicals

Table 2. Reaction steps used for modeling aqueous radical polymerization of acrylic acid.

Initiator kinetics		
Initiator decomposition	$S_2O_8^{2-} \xrightarrow{k_d} 2SO_4^{\bullet-}$	(2)
Chain initiation	$SO_4^{\bullet-} + AA \xrightarrow{k_{p,I}} R_{sec}^{\bullet}(o,o)$	(3)
SPR kinetics		
Propagation of SPRs	$R_{sec}^{\bullet}(s,l) + AA \xrightarrow{k_{p,sec}} R_{sec}^{\bullet}(s,l)$	(4)
SPR–SPR termination	$R_{sec}^{\bullet}(s,l) + R_{sec}^{\bullet}(m,r) \xrightarrow{k_{tc}} P_n(s+m,l+r)$	(5)
CTA kinetics		
Transfer to CTA	$R_{sec}^{\bullet}(s,l) + CTA \xrightarrow{k_{f,CTA}} R_{CTA}^{\bullet} + P_n(s,l)$	(6)
Redox decomposition	$S_2O_8^{2-} + CTA(RSH) \xrightarrow{k_r} SO_4^{\bullet-} + R_{CTA}^{\bullet}(RS^{\bullet}) + HSO_4^-$	(7)
CTA initiation	$SO_4^{\bullet-} + CTA \xrightarrow{k_{f,CTA}} R_{CTA}^{\bullet} + HSO_4^-$	(8)
CTA propagation	$R_{CTA}^{\bullet} + AA \xrightarrow{k_{p,CTA}} R_{sec}^{\bullet}(o,o)$	(9)
MCR kinetics		
Backbiting	$R_{sec}^{\bullet}(s,l) \xrightarrow{k_{bb}} R_{tert}^{\bullet}(s+1,l)$	(10)
Intermolecular transfer	$R_{sec}^{\bullet}(m,r) + P_n(s,l) \xrightarrow{k_{f,p}} P_n(m,r) + R_{tert}^{\bullet}(s,l+1)$	(11)
Propagation	$R_{tert}^{\bullet}(s,l) + AA \xrightarrow{k_{p,tert}} R_{sec}^{\bullet}(s,l)$	(12)
MCR-SPR termination	$R_{tert}^{\bullet}(s,l) + R_{sec}^{\bullet}(m,r) \xrightarrow{k_{tc}} P_n(s+m,l+r)$	(13)

The main model assumptions are: 1) isothermal semibatch polymerization in dilute solution, 2) decomposition of KPS via thermal and acid catalyzed routes (the last one does not produce free radicals),[29] 3) AA only consumed by propagation reactions (long-chain hypothesis), 4) propagation rate constant of AA independent of AA concentration in dilute aqueous solution, 5) radicals termination by combination with an unique constant rate independently of the radical nature, 6) generation of $R_{tert}^{\bullet}$ and of a new long-chain branch by intermolecular H abstraction from the tertiary Carbon on the polymer chain, 7) generation of $R_{tert}^{\bullet}$ and of a new short-chain branch by intramolecular H abstraction from tertiary Carbon on the growing macroradicals, 8) different propagation rate constants for $R_{sec}^{\bullet}$, $R_{tert}^{\bullet}$ and CTA radicals, agreeing with those observed by pulsed laser polymerization (PLP)-SEC, where $R_{tert}^{\bullet}$ exhibits a lower reactivity than $R_{sec}^{\bullet}$,[30] 9) pseudo-stationary state for all radical species, 10) rate constants are not diffusion controlled and are independent of the chain length, 11) negligible transfer to monomer, and 12) the reaction media is considered as a weak acids mixture for pH estimation. The full mathematical model is presented in the Appendix.

by reaction of sulfate radicals with CTA (Equation (8)), vii) propagation of CTA radicals produced by Equations (6–9), viii) intramolecular H transfer (backbiting), generating more stable radicals, meaning that the radical end (secondary radical) isomerizes to an internal position (tertiary radical) during propagation, giving place to a new short branch point (Equation (10)); ix) intermolecular transfer to the polymer produced by the abstraction of a tertiary H of PAA, where tertiary radicals are generated in the polymer chain, thus generating a new long branch point (Equation (11)), x) propagation of tertiary radicals with AA (Equation (12)); and xi) termination of SPR and MCR by bimolecular combination (Equation (13)), and termination by disproportionation[12,18] between two MCR,[11] and (intra and inter-) abstraction of $R_{tert}^{\bullet}$ negligible. Note that in Equation (8) some sulfate radicals are deactivated by transferring the radical function to the –SH ending CTA, thus generating a new radical $R_{CTA}^{\bullet}$ that can also initiate propagation by reacting with a monomer molecule in Equation (9) (thiol-ene reaction).

Most of the model parameters were adopted from literature, while the rate constants of transfer to polymer ($k_{f,p}$), transfer to TGA ($K_{f,CTA}$), CTA radicals propagation ($K_{p,CTA}$), and redox decomposition of SH–CTAs with KPS (k_r) were adjusted to fit the experimental data of x_f, $\bar{M}_n$, and $\bar{M}_w$. The parameters are summarized in Table 3.

Macromol. React. Eng. **2017**, DOI: 10.1002/mren.201600049

Table 3. Model parameters employed to fit the experimental data (at 70 °C).

Constant	CTA	Value	References
f (–)		0.5	[18]
k_d(min^{-1})		8.83×10^{-3}	[18]
$k_{p,sec}$(L mol^{-1} min^{-1})		3.51×10^{7}	[31]
k_{tc}(L mol^{-1} min^{-1})		4.48×10^{11}	[11]
$k_{p,CTA}$(L mol^{-1} min^{-1})	ME	3.51×10^{7}	This work
	TGA	1.57×10^{7}	This work
	IPA	3.51×10^{7}	This work
$C_{f,CTA}$(–)	ME	2.8×10^{-1}	[32]
	TGA	1.9×10^{-1}	This work
	IPA	3.1×10^{-4}	[33]
k_r(L mol^{-1} min^{-1})	ME	5.00×10^{2}	This work
	TGA	1.96×10^{2}	This work
k_{bb}(min^{-1})		9.58×10^{4}	[32]
$k_{f,p}$(L mol^{-1} min^{-1})		5.50×10^{2}	This work
$k_{p,tert}$(L mol^{-1} min^{-1})		2.46×10^{5}	This work
H+ Dissociation Constants			
K_{AA}(mol L^{-1})	AA	5.52×10^{-5}	[34]
K_{PAA}(mol L^{-1})	PAA	1.0×10^{-5}	[34]
K_{ME}(mol L^{-1})	ME	1.9×10^{-10}	[34]
K_{TGA}(mol L^{-1})	TGA	2.3×10^{-4} (COOH)	[34]
		2.5×10^{-11} (SH)	
K_{IPA}(mol L^{-1})	IPA	1.1×10^{-18}	[35]

4. Results and Discussion

Hereinafter, the effect of including each CTA (ME, TGA, or IPA), on the aqueous solution polymerization of AA carried out under semicontinuous conditions with varied feed periods and reaction times is considered. For all experiments, the bottom part of Table 1 summarizes the final values of x, $\bar{M}_n$, $\bar{M}_w$, polydispersity (D_n), and pH.

4.1. Semicontinuous Polymerization of AA in the Presence of ME

Figure 1 compares the experimental and simulated evolutions of x_f, pH, $\bar{M}_n$, and . for CR and ME-based experiments. In CR, bimolecular termination mainly controls the MM.[18] The incorporation of ME contributes to reduce the MM. Thus, reaction ME1 reduces 50% the $\bar{M}_n$ and $\bar{M}_w$ values obtained in CR, without affecting the AA conversion. This indicates that the chain transfer to ME importantly contributes to control MM and that the transferred radicals($R^{\bullet}_{CTA}$) are able to propagate. However, the increment of the ME concentration in ME2 did not produce a further reduction of the MM, while the AA conversion was meaningfully reduced. Even though the reaction time was extended for 30 min after the feeding period, the AA conversion remained relatively low. In ME3, the reduction of both KPS and ME concentration with respect to ME2 produced MM similar to those of CR. This is because the reduction of KPS concentration decreases both the radical concentration and the termination rate, which compensates for the MM reduction due to the chain transfer to CTA. These observations are confirmed by the MMDs of final samples (Figure 2), where: (i) the MMD is shifted toward lower MM when ME is incorporated (ME1 and ME2), and (ii) broader MMD with respect to CR is observed in ME3, due to the opposite effect between the lower termination and the presence of CTA, which is not able to completely control de MMD. Notice that the incorporation of ME in ME2 and ME3 reduced the final AA conversion, but this effect is only apparent in the last stage of the process.

The mathematical model reasonably predicts the evolution of x_f, $\bar{M}_n$, $\bar{M}_w$, and pH of reactions with ME and of CR (Figure 1). The main cause of the incomplete AA polymerization by the presence of ME (in experiments

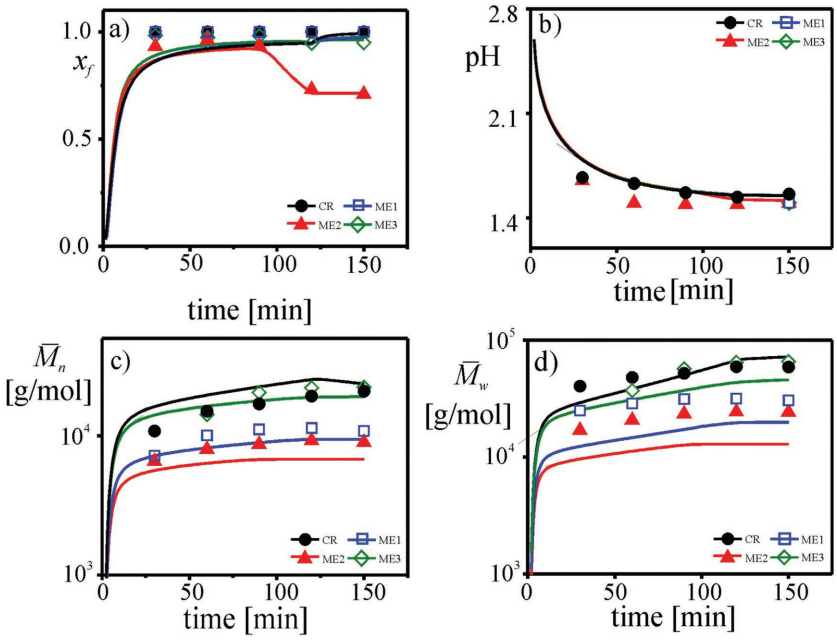

Figure 1. Semibatch polymerization of AA in the presence of ME (in comparison with the CR experiment). a–d) Evolutions of x_f, pH, $\bar{M}_n$, and $\bar{M}_w$. Experimental data (symbols) and simulation results (curves).

ME2 and ME3), is the capability of the SH–CTA to act as reducing agent with KPS. Thus, the resulting redox initiation SH–CTA/KPS not only promotes the production of primary radicals, but also increases the consumption of KPS. Figure 3 compares the model prediction for KPS concentration during the experiments in presence of ME (ME1-3), with that obtained when only thermal decomposition is present (CR). Even though KPS is always present during the CR reaction, it is completely consumed before the reaction end in the experiments with ME, thus producing the important fall in the polymerization rate observed in Figure 1a. Since AA is continuously fed during the polymerization (with $t_{feeding}$ = 120 min), then the time at which the KPS is totally consumed practically determines the final AA conversion. According to simulation, KPS disappears in ME2 at 80 min (66.7% of the $t_{feeding}$), reaching a final conversion of 73.5%. On the contrary, in ME1 and ME3, KPS is available until the end of the feeding stage and, for this reason, a significant inhibition is not observed.

Notice that fractional AA conversion was close to 1 when the polymerization proceeds in presence of KPS (before inhibition), which indicates that AA concentration was low along the reaction. For this reason, in these semibatch experiments the propagation rate constant was assumed to be independent of the AA concentration, without deteriorating the prediction of x_f.

The gel phase ^{13}C NMR of the final sample of experiment ME2 (Figure 4) confirms the formation of $R^{\bullet}_{CTA}$. The peak at 57.6 ppm shows the carbon linked to the alcohol group at the end of the polymer chain, which corresponds to the propagation of the radical $^{\bullet}SCH_2CH_2OH$ from ME.

A quaternary carbon peak (Cq) is observed in the ^{13}C NMR spectrum (Figure 4), at 47.2 ppm which indicates the occurrence of both inter- and intramolecular H abstraction. The calculated BD determined from NMR information (Equation (1)), the model predictions of BD, and its short (BD_s) and long (BD_l) branching contributions, are summarized in Table 4. According to the model prediction, the main branching mechanism is due to intramolecular

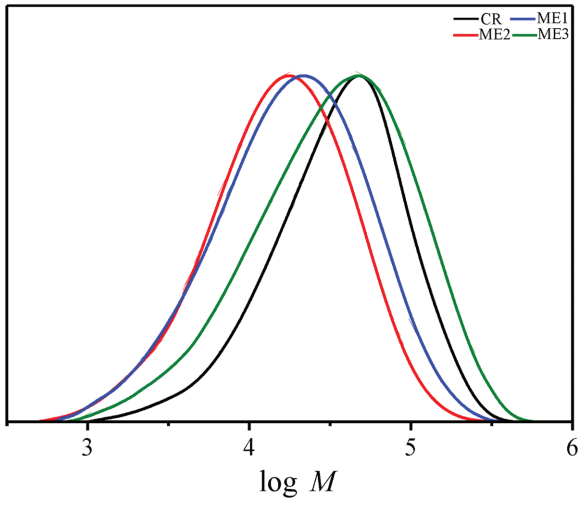

Figure 2. MMD of the final PAA samples obtained in experiments with ME (in comparison with the CR experiment).

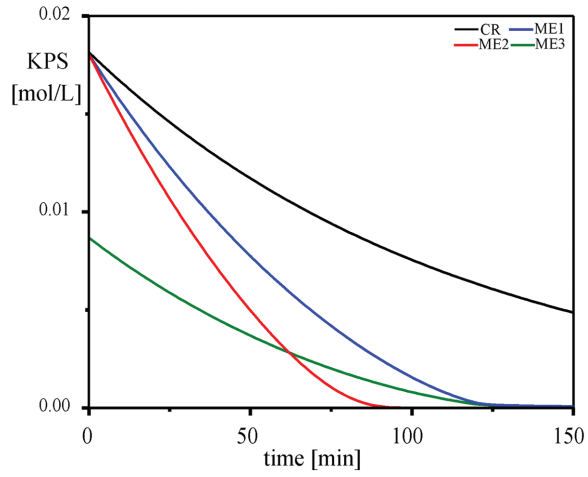

Figure 3. Model prediction for the evolution of the KPS concentration. Comparison between ME1-3 and CR experiments.

Macromol. React. Eng. **2017**, DOI: 10.1002/mren.201600049

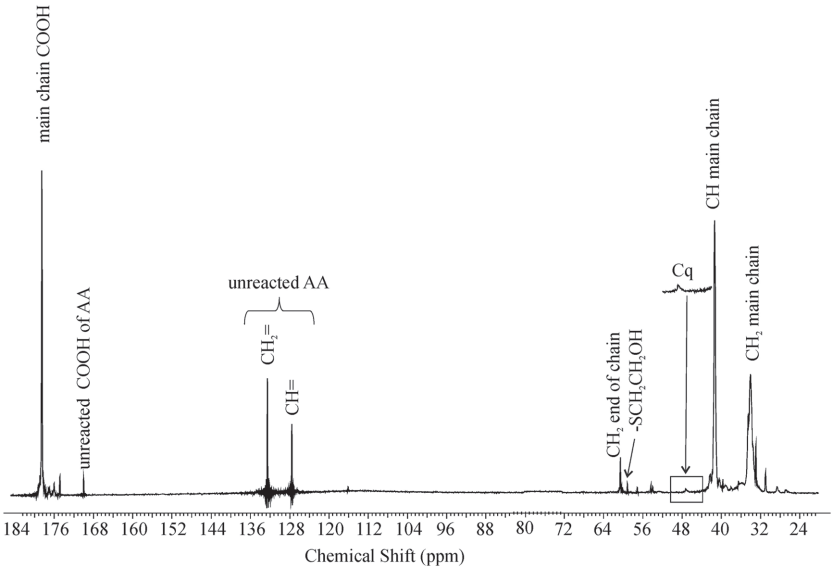

Figure 4. ^{13}C NMR spectrum of the final product obtained in the ME2 experiment.

H abstraction (short branches are around 100-fold in number over long branches), in agreement with previous reports.[18,32] However, long branches have an important effect on polymer structure, and they must be taken into account to adequately fit the experimental $\bar{M}_w$ data.

The incorporation of ME produces an increment in BD with respect to CR. The main mechanism for increasing short branching (Equation (A.8)) in the presence of ME is the higher radical generation obtained as a consequence of the redox initiation mechanism between ME and KPS (Equation (7)). Figure 3 clearly shows the faster KPS consumption (i.e., the faster radicals generation) when ME is present in comparison with that of CR.

The pH values of all final samples are lower than 2.15 or 1.91 (i.e., the values which correspond to a 20% aqueous solution of PAA or AA; see bottom of Table 1). The proposed model adequately predicts the evolution of pH in experiment CR (Figure 1b), thus suggesting that a fraction of KPS generates sulfuric acid according the mechanism of Table 2.[29] Notice that the final pHs of reactions with ME are similar to that of CR, because ME is a weak acid with a negligible contribution of H^+.

Table 4. Comparison between experimental and simulated BD for final PAA samples of all experiments.

Experiment	^{13}C NMR measurements	Simulation results		
	BD [%]	BD [%]	BD_s [%]	BD_l [%]
CR	2.7	1.97	1.96	0.01
ME1	3.1	2.45	2.43	0.02
ME2	4.2	2.63	2.61	0.02
ME3	3.1	2.05	2.03	0.02
TGA1	2.9	2.79	2.77	0.02
TGA2	1.5	2.36	2.36	0.02
TGA3	1.0	1.93	1.91	0.02
IPA1	3.8	2.00	1.99	0.01
IPA2	5.2	1.99	1.98	0.01

4.2. Semicontinuous Polymerization of AA in the Presence of TGA

The incorporation of TGA (TGA1-3) importantly reduces the MMs with respect to CR (Table 1 and Figure 5). Also, the presence of TGA importantly affects the AA conversion, depending not only on the CTA concentration, but also on the feeding time. When both the feeding and the reaction times are reduced, while maintaining constant the CTA/AA ratio, higher MMs are obtained, but lower inhibitions and higher final conversions are observed (TGA1-3). In CR, $\bar{M}_n$ and $\bar{M}_w$ increase along the reaction, as a consequence of the radical concentration reduction, together with the occurrence of chain transfer to the polymer, which is more important at the end of the process.[28] When the feeding time is reduced, the AA concentration is increased, the polymerization becomes faster and, therefore, the inhibition is less important and appreciable (Figure 5 and Table 1).

Figure 6 shows the model prediction of the KPS concentration during TGA experiments compared with that of the CR experiment. In TGA experiments, KPS runs out simultaneously with the beginning of the observed inhibition period (Figure 5a), due to the redox initiation between KPS and TGA (Equation (7)). Also, when $t_{feeding}$ is decreased (from TGA1 to TGA3) a shorter period of polymerization proceeds in absence of KPS. For each polymerization, the corresponding $t_{feeding}$ is indicated with an arrow in the abscissa of Figure 6.

When the feeding rate is increased (or equivalently, the $t_{feeding}$ is decreased), then higher MMs are obtained. This is because a larger amount of AA is polymerized while maintaining constant the flux of radicals in all cases (KPS runs out before $t_{feeding}$), and the relationship between the transfer rate constant to the TGA and the propagation rate constant of AA is lower than one ($C_{f,TGA} = 0.19$). The opposite effect of feeding rate on BD was observed in Table 4. In fact, BD decreased with feeding rate due to the lower probability of chain transfer to polymer and backbiting reactions with respect to propagation when the amount of polymerized AA was increased, while maintaining

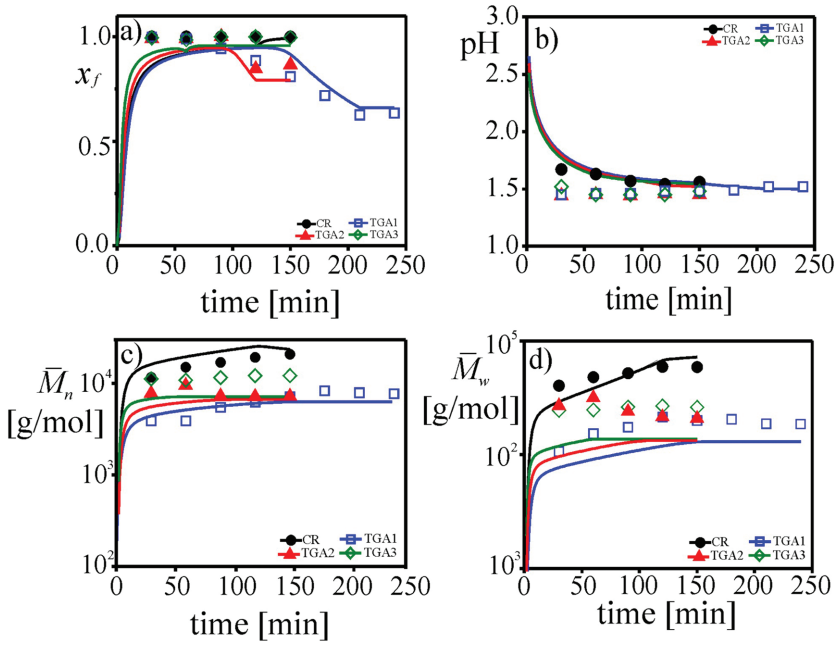

Figure 5. Polymerization of AA in the presence of TGA and its comparison with the CR experiment. a–d) Evolutions of x_f, pH, $\bar{M}_n$, and $\bar{M}_w$. Experimental data (symbols) and simulation results (curves).

constant the flux of radicals. In conclusion, as the feeding rate increases, the propagation is promoted without practically changing termination, chain transfers, and backbiting reactions.

Notice that experiments ME2 and TGA2 employed the same CTA/AA molar ratio. In TGA2, lower MMs and less inhibition (higher final conversions) were observed with respect to ME2. These observations were also predicted by the model, where the adjusted values of the redox initiation constant rate SH–CTA/KPS (k_r) for ME was higher than for TGA, thus indicating a greater inhibition and lower availability of CTA when ME is used.

Finally, for experiments that involved TGA, the pHs were lower than for CR and ME experiments (see bottom of Table 1 and Figure 5b). This is because TGA is a stronger acid than AA and PAA (see bottom of Table 3). These results were well predicted by the model, through the overall balance of protons.

4.3. Semicontinuous Polymerization of AA in the Presence of IPA

Figure 7 shows the evolution of x_f, pH, $\bar{M}_n$ and $\bar{M}_w$, along the polymerization, with the incorporation of IPA as CTA (IPA1,2), in comparison to the CR experiment. For the same CTA/AA molar ratio, the MMs obtained in IPA1 were higher than with ME and TGA (see experiments ME2 and TGA1), thus indicating that IPA has a lower chain transfer capability. This is also confirmed by the adopted $k_{f,CTA}$ values of Table 3.[32] To achieve a meaningful reduction in the MMs, the CTA initial concentration in IPA2 was ten times higher than in IPA1. Figure 8 shows the MM distributions for experiments IPA1 and IPA2. Notice that the MMs of the obtained PAA were little affected (in comparison to the CR experiment).

Also, in the reactions where IPA was used as CTA, the fractional conversions reached 100%, and their evolutions were coincident with that of CR. This suggests that the only source of KPS consumption is the thermal decomposition. For this reason, the KPS concentration exhibits an evolution superimposed with that of CR. IPA is a weak acid and therefore, for low CTA concentrations, the pH was not further reduced with respect to that of CR. However, when a high amount of IPA was fed, lower pH values were obtained (Table 1 and Figure 7). Finally, a significant effect on BD was not observed when IPA was used, because the absence of thiol groups in this CTA does not interfere in the radical generation.

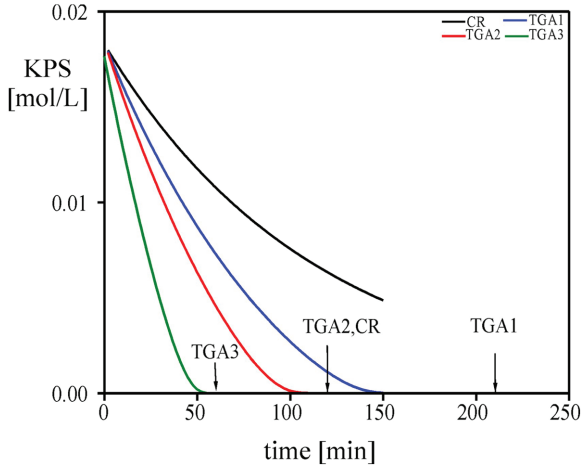

Figure 6. Model predictions for the evolution of the KPS concentration in TGA experiments compared to the CR experiment (the arrows for each experiment indicate the end of the feeding period).

5. Conclusions

The semibatch aqueous solution polymerization of nonionized AA at 70 °C with the addition of ME, TGA, or IPA as CTA was investigated, with the objective of producing low molar mass PAAs, in a process operating under safe isothermal conditions. With proper selection of the amount of CTA and the feeding time, PAAs of relatively low MM

Macromol. React. Eng. **2017**, DOI: 10.1002/mren.201600049

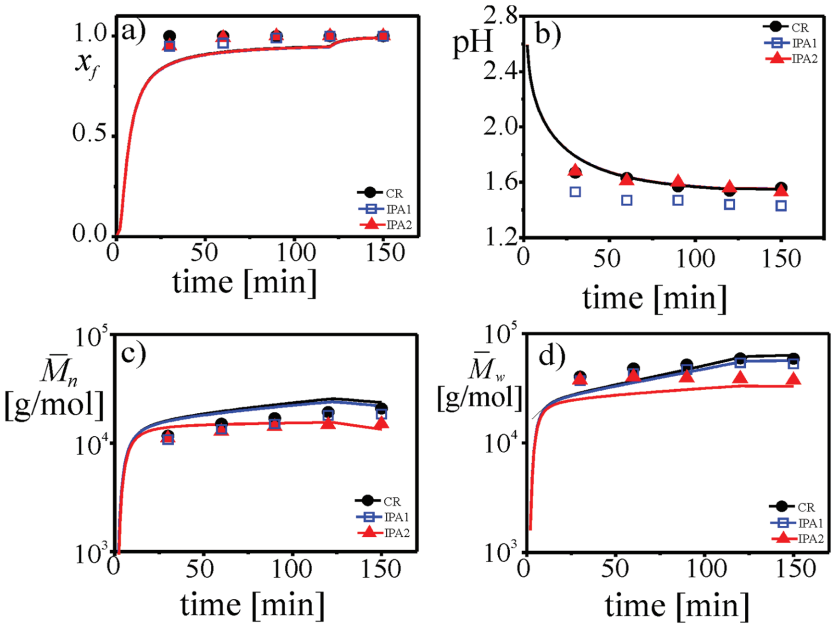

Figure 7. Polymerization of AA in the presence of IPA and its comparison with the CR experiment. a–d) Evolutions of x_f, pH, $\bar{M}_n$, and $\bar{M}_w$. Experimental data (symbols) and simulation results (curves).

($\bar{M}_n \approx 10.8$ kDa with ME, $\bar{M}_n \approx 12.1$ kDa with TGA, and $\bar{M}_n \approx 15.1$ kDa with IPA) can be synthesized, at conversion close to 100%. In contrast, larger MMs were obtained in absence of CTA ($\bar{M}_n \approx 20.9$ kDa) under equivalent experimental reaction conditions. With higher concentration of either ME or TGA, PAA with lower MMs could be obtained, but without reaching complete AA conversion under the investigated conditions.

Lower feeding rates of AA and TGA, and higher mercaptan (ME and TGA) concentrations, adversely affect the fractional conversion, because KPS is more quickly consumed by the KPS/SH–CTA redox system. This effect is more important than the thermal decomposition of KPS in Equation (2) ($k_r > k_d$), and tends to rapidly stop the polymerization. Also, the increment of both the feeding time and the concentration of SH–CTA in TGA and ME respectively, adversely affect the BD of PAA, because radical generation is promoted.

For similar reaction conditions, the IPA has a lower effect than other CTAs. It does not participate in the initiation process, and therefore x_f is almost unaffected. Also, for equimolar CTA concentration, TGA produced PAA of lower MM and higher conversions.

The proposed mathematical model for semibatch reactions was able to adequately predict the inhibition effects and the molecular architecture of PAA due to the presence of CTA, and the evolution of main measured variables. This was reached even when using simple parameters, independent of pH, AA, and polymer concentrations.

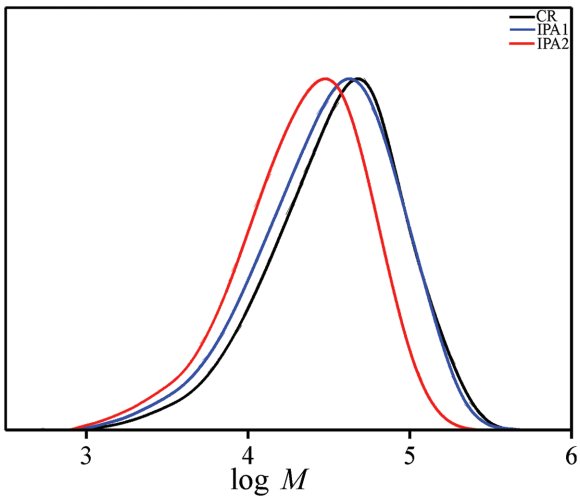

Figure 8. Molar mass distributions of final PAA samples obtained in the IPA experiments (IPA1, IPA2) compared to the CR experiment.

5.1. Mathematical Model for the Aqueous-Solution Polymerization of AA in presence of a Chain Transfer Agent

Based on the model by Minari et al.[18] and from the kinetic considerations and hypothesis previously described in the kinetics and mathematical model section, the following balances can be written

$$\frac{dN_{AA}}{dt} = F_{AA} - R_p V \quad (A.1)$$

$$\frac{dN_{KPS}}{dt} = -(k_d([KPS] + k_r[KPS][CTA])V \quad (A.2)$$

$$\frac{dN_{CTA}}{dt} = F_{CTA} - (k_{f,CTA}[CTA][R^\bullet] + k_r[KPS][CTA])V \quad (A.3)$$

$$\frac{dV}{dt} = F_w v_w + F_{AA} v_{AA} + F_{CTA} v_{CTA} \quad (A.4)$$

$$\frac{d(Q_o V)}{dt} = \left(\tau + \frac{\beta}{2}\right) R_p V \quad (A.5)$$

$$\frac{d(Q_1 V)}{dt} = R_p V \quad (A.6)$$

$$\frac{d(Q_2 V)}{dt} = \left[1 + C_{f,CTA}\frac{[CTA]}{[AA]} + 2\left(\frac{A}{B}\right) + \beta\left(\frac{A}{B}\right)^2\right] R_p V \quad (A.7)$$

$$\frac{d(BD_s Q_1 V)}{dt} = k_{bb}[R^{\bullet}_{sec}]V \quad (A.8)$$

$$\frac{d(BD_l Q_1 V)}{dt} = k_{f,p}[R^{\bullet}_{sec}]Q_1 V \quad (A.9)$$

with

$$[i] = \frac{N_i}{V};\ (i = AA, KPS, CTA) \quad (A.10)$$

$$R_p = \left(k_{p,sec}[R^{\bullet}_{sec}] + k_{p,tert}[R^{\bullet}_{tert}] + k_{p,CTA}[R^{\bullet}_{CTA}]\right)[AA] \quad (A.11)$$

$$\beta = \frac{k_{tc}[R^{\bullet}]^2}{k_{p,sec}[R^{\bullet}_{sec}][AA] + k_{p,tert}[R^{\bullet}_{tert}][AA] + k_{p,CTA}[R^{\bullet}_{CTA}][AA]} \quad (A.12)$$

$$\tau = \frac{k_{td}[R^{\bullet}]^2 + k_{f,m}[R^{\bullet}][AA] + k_{fx}[R^{\bullet}][CTA]}{k_{p,sec}[R^{\bullet}_{sec}][AA] + k_{p,tert}[R^{\bullet}_{tert}][AA] + k_{p,CTA}[R^{\bullet}_{CTA}][AA]} \quad (A.13)$$

$$C_{f,CTA} = \frac{k_{f,CTA}}{k_{p,sec}} \quad (A.14)$$

$$C_{f,p} = \frac{k_{f,p}}{k_{p,sec}} \quad (A.15)$$

$$A = \left(1 + \frac{k_{f,m}[R^{\bullet}_{sec}][AA] + k_{fp}Q_2[R^{\bullet}] + k_{f,CTA}[R^{\bullet}][CTA]}{k_{p,sec}[R^{\bullet}_{sec}][AA] + k_{p,tert}[R^{\bullet}_{tert}][AA] + k_{p,CTA}[R^{\bullet}_{CTA}][AA]}\right) \quad (A.16)$$

$$B = \left(\tau + \beta + \frac{C_{f,p}[R^{\bullet}_{sec}]Q_1}{k_{p,sec}[R^{\bullet}_{sec}][AA] + k_{p,tert}[R^{\bullet}_{tert}][AA] + k_{p,CTA}[R^{\bullet}_{CTA}][AA]}\right) \quad (A.17)$$

where N_{AA} and N_{KPS} are the moles of AA and KPS, respectively; F_{AA}, F_{CTA}, and F_w are the molar AA, CTA, and water feed rates; V is the total reaction volume; v_{AA}, v_{CTA}, and v_w are the molar volumes of AA, CTA, and water, at the reaction temperature; Q_0, Q_1, and Q_2 are the first three moments of the number chain-length distribution, $[i]$ is the molar concentration of specie i; and BD_s and BD_l are the branching degrees due to short and long branches, respectively.

The radical concentrations $[R^{\bullet}]$, $[R^{\bullet}_{CTA}]$, $[R^{\bullet}_{tert}]$, and $[R^{\bullet}_{sec}]$, are calculated according to

$$[R^{\bullet}] = \sqrt{\frac{f k_d[KPS] + k_r[KPS][CTA]}{k_{tc}}} \quad (A.18)$$

$$\left[R^{\bullet}_{tert}\right] = \frac{k_{bb}[R^{\bullet}_{sec}]}{k_{p,tert}[AA]} \quad (A.19)$$

$$\left[R^{\bullet}_{CTA}\right] = \frac{k_{f,CTA}[R^{\bullet}_{sec}][CTA] + k_r[KPS][CTA]}{k_{p,CTA}[AA]} \quad (A.20)$$

$$[R^{\bullet}_{sec}] = [R^{\bullet}] - [R^{\bullet}_{CTA}] - [R^{\bullet}_{tert}] \quad (A.21)$$

Fractional (x_f) and global (x) conversions are estimated by:

$$x_f(t) = \frac{N^{\circ}_{AA} + \int_0^t F_{AA}\,dt - N_{AA}(t)}{N^{\circ}_{AA} + \int_0^t F_{AA}\,dt} \quad (A.22)$$

$$x(t) = \frac{N^{\circ}_{AA} + \int_0^{DT} F_{AA}\,dt - N_{AA}(t)}{N^{\circ}_{AA} + \int_0^{DT} F_{AA}\,dt} \quad (A.23)$$

where N°_{AA} represents the initial load of AA (zero in our experiments) and DT is the feeding time of the reagents.

Finally, the average MMs and the total BD are calculated from:

$$\bar{M}_n = M_{AA}\frac{Q_1}{Q_0} \quad (A.24)$$

$$\bar{M}_w = M_{AA}\frac{Q_2}{Q_1} \quad (A.25)$$

$$BD = BD_l + BD_s \quad (A.26)$$

where M_{AA} represents the MM of AA.

Calculation of $[H^{\pm}]$.

The $[H^+]$ was calculated by considering that there is a mixture of weak acids in the reactor, and taking into account the contributions of all acid species present (AA and PAA for each used CTA: ME, TGA, and IPA)[36] and the generation of H_2SO_4 from the KPS initiator[29] that follow a kinetic of pseudo first order.[37]

$$\left[H^+\right] = 2.32\times10^{-2}(1-\exp(-0.025t)) + \sqrt{K_{AA}[AA] + K_{CTA}[CTA] + K_{PAA}[PAA] + 1\times10^{-14}} \quad (A.27)$$

$$pH = -\log[H^+] \quad (A.28)$$

Acknowledgements: The authors are grateful to ANPCyT, CONICET, and UNL (Argentina) for the financial support of this work.

Received: August 11, 2016; Revised: November 17, 2016; Published online: ; DOI: 10.1002/mren.201600049

Keywords: chain transfer agent; molar mass distribution; poly(acrylic acid)

[1] A. Laguecir, S. Ulrich, J. Labille, N. Fatin-Rouge, S. Stoll, J. Buffle, *Eur. Polym. J.* **2006**, *42*, 1135.
[2] A. Dobrynin, M. Rubinstein, *Prog. Polym. Sci.* **2005**, *30*, 1049.
[3] J. Sarraguça, A. Pais, *Chem. Phys. Lett.* **2004**, *398*, 140.
[4] F. Demir, *Appl. Clay Sci.* **2015**, *105–106*, 41.
[5] F. Buchholz, in *Ullmann's Encyclopedia of Industrial Chemistry*, Vol. *A21* (Eds. B. Elvers, S. Hawkins, G. Schulz), VCH Weinheim, Germany **1992**.
[6] G. Gratzl, S. Walkner, S. Hild, A. Hassel, H. Weber, C. Paulik, *Colloids Surf., B* **2015**, *126*, 98.
[7] A. Sarkar, A. Pal, S. Ghorai, N. Mandre, S. Pal, *Carbohydr. Polym.* **2014**, *111*, 108.
[8] E. Abdel-Halim, S. Al-Deyab, *React. Funct. Polym.* **2014**, *75*, 1.
[9] J. Iqbal, C. Vigl, G. Moser, M. Gasteiger, G. Pereral, A. Bernkop-Schnürch, *Drug Deliv ery* **2011**, *18*, 432.
[10] S. Jha, K. Hayashi, *Sens. Actuators, B.* **2015**, *206*, 471.
[11] J. Barth, M. Buback, W. Meiser, *Macromol ecules* **2012**, *45*, 1339.
[12] R. Scott, N. Peppas, *AIChE J.* **1997**, *43*, 135.
[13] T. Liu, B. Qian, J. Li, K. Zhu, H. Deng, X. Yang, X. Wang, *Carbohydr. Polym.* **2013**, *94*, 261.
[14] T. Wu, T. Xie, G. Yang, *J. Polym. Sci., Part B: Polym. Phys.* **2008**, *46*, 2335.
[15] J. Loiseau, N. Doerr, J. Suau, J. Egraz, M. Llauro, C. Ladaviere, *Macromolecules* **2003**, *36*, 3066.
[16] M. Chevrel, N. Brun, S. Hoppe, D. Meimaroglou, L. Falk, D. Chapron, A. Durand, *Chem Eng. Sci.* **2014**, *106*, 242.
[17] P. Deglmann, I. Müller, F. Becker, A. Schäfer, K.-D. Hungenberg, H. Weiß, *Macromol. React. Eng.* **2009**, *3*, 496.
[18] R. Minari, G. Cáceres, P. Mandelli, M. Yossen, M. Gonzalez-Sierra, J. Vega, L. Gugliotta, *Macromol. React. Eng.* **2011**, *5*, 223.
[19] T. Spychaj, *Prog. Org. Coat.* **1989**, *17*, 71.
[20] J. Cramm, K. Bailey (Nalco Chemical Company) US. Patent 4698404, **1987**.
[21] F. Ehlers, J. Barth, P. Vana, *Fundamentals of Controlled/Living Radical Polymerization* (Eds: N. Tsarevsky, B. Sumerlin), RSC, London **2013**, p. 20.
[22] N. Wittenberg, *Doctor Thesis*, Georg-August-Universität Göttingen **2013**.
[23] M. Graeme, D. Solomon, *The Chemistry of Radical Polymerization* 2nd ed., Elsevier Sci, The Netherlands **2006**, Ch. 6, p. 279.
[24] S. Maiti, R. Palit, *J. Polym. Sci. Part A-1: Polym. Chem.* **1971**, *9*, 253.
[25] G. Misra, U. Bajpai, *Prog. Polym. Sci.* **1982**, *8*, 61.
[26] G. Bokias, A. Durand, D. Hourdet, *Macromol. Chem. Phys.* **1998**, *199*, 1387.
[27] M. Zammit, T. Davis, K. Suddaby, *Polymer* **1998**, *39*, 5789.
[28] A. Sarac, *Prog. Polym. Sci.* **1999**, *24*, 1149.
[29] M. Kolthoff, I. Miller, *J. Am. Chem. Soc.* **1951**, *73*, 3055.
[30] M. Buback, P. Hesse, I. Lacik, *Maromol. Rapid. Commun.* **2007**, *28*, 2049.
[31] I. Lacík, S. Beuermann, M. Buback, *Macromolecules* **2003**, *36*, 9355.
[32] N. Wittenberg, C. Preusser, H. Kattner, M. Stach, I. Lacík, R. Hutchinson, M. Buback, *Macromol. React. Eng.* **2015**, *10*, 95.
[33] K. Anda, S. Iwai, K. Kobunshi, in *Polymer Handbook*, (Eds: J. Brandrup, E. H. Immergut), 3rd ed., Wiley, New York **1989**, p. II/110.
[34] California State University Northridge, www.csun.edu/~hcchm003/321/Ka.pdf (accessed: August 2011).
[35] D. Mackay, W. Shiu, Y. Ma, C. Lee, *Handbook of Physical-Chemical Properties and Environmental Fate for Organic Chemicals*, 2nd ed., Taylor & Francis, USA **2006**, p. 2491.
[36] D. Harris, *Quantitative chemical analysis*, 8th ed., W.H. Freeman and Co., New York **2010**, p. 181.
[37] S. Logan, J. Rodríguez, *Fundamentos de Cinética Química*, Addison-Wesley Iberoamericana España, S.A. **1999**, p. 89.